HAL
open science

The impact of SCIAMACHY near-infrared instrument calibration on CH4 and CO total columns

A. M. S. Gloudemans, H. Schrijver, Q. Kleipool, M. M. P. van den Broek, A. G. Straume, G. Lichtenberg, R. M. van Hees, I. Aben, J. F. Meirink

To cite this version:

A. M. S. Gloudemans, H. Schrijver, Q. Kleipool, M. M. P. van den Broek, A. G. Straume, et al.. The impact of SCIAMACHY near-infrared instrument calibration on CH4 and CO total columns. Atmospheric Chemistry and Physics Discussions, 2005, 5 (2), pp.1733-1770. hal-00301109

HAL Id: hal-00301109

https://hal.science/hal-00301109v1

Submitted on 18 Jun 2008

HAL is a multi-disciplinary open access archive for the deposit and dissemination of scientific research documents, whether they are published or not. The documents may come from teaching and research institutions in France or abroad, or from public or private research centers.

L'archive ouverte pluridisciplinaire **HAL**, est destinée au dépôt et à la diffusion de documents scientifiques de niveau recherche, publiés ou non, émanant des établissements d'enseignement et de recherche français ou étrangers, des laboratoires publics ou privés.

Atmos. Chem. Phys. Discuss., 5, 1733–1770, 2005
www.atmos-chem-phys.org/acpd/5/1733/
SRef-ID: 1680-7375/acpd/2005-5-1733
European Geosciences Union

Atmospheric Chemistry and Physics Discussions

The impact of SCIAMACHY near-infrared instrument calibration on CH_4 and CO total columns

A. M. S. Gloudemans[1], H. Schrijver[1], Q. Kleipool[1,*], M. M. P. van den Broek[1], A. G. Straume[1,], G. Lichtenberg[1], R. M. van Hees[1], I. Aben[1], and J. F. Meirink[2]**

[1]SRON National Institute for Space Research, Utrecht, The Netherlands
[2]Royal Netherlands Meteorological Institute (KNMI), De Bilt, The Netherlands
[*]now at: Royal Netherlands Meteorological Institute (KNMI), De Bilt, The Netherlands
[**]now at: the European Space Agency, European Space Research & Technology Centre (ESA-ESTEC), Noordwijk, The Netherlands

Received: 9 February 2005 – Accepted: 3 March 2005 – Published: 18 March 2005

Correspondence to: A. M. S. Gloudemans (a.gloudemans@sron.nl)

© 2005 Author(s). This work is licensed under a Creative Commons License.

Abstract

The effects of three important SCIAMACHY near-infrared instrument calibration issues on the retrieved methane (CH_4) and carbon monoxide (CO) total columns have been investigated: the effects of the growing ice layer on the near-infrared detectors, the effects of the orbital variation of the instrument dark signal, and the effects of the dead/bad detector pixels. Corrections for each of these instrument calibration issues have been defined. The retrieved CH_4 and CO total columns including these corrections show good agreement with CO measurements from the MOPITT satellite instrument and with CH_4 model calculations by the chemistry transport model TM3. Using a systematic approach, it is shown that all three instrument calibration issues have a significant effect on the retrieved CH_4 and CO total columns, although the impact on the CH_4 total columns is more pronounced than for CO. Results for three different wavelength ranges are compared and show good agreement. The growing ice layer and the orbital variation of the dark signal show a systematic, but time-dependent effect on the retrieved CH_4 and CO total columns, whereas the dead/bad pixels show a more random effect. The importance of accurate corrections for each of these instrument calibration issues is illustrated using examples where inaccurate corrections lead to a wrong interpretation of the results.

1. Introduction

The SCanning Imaging Absorption spectroMeter for Atmospheric CHartographY (SCIAMACHY)[1] which was launched on board the ENVISAT satellite on 1 March 2002, has allowed the measurement of global distributions of methane (CH_4) and carbon monoxide (CO) down to the Earth's surface. These gases play an important role in tropospheric chemistry and possible climate change. Therefore, a good knowledge of

[1] http://envisat.esa.int/instruments/sciamachy/

the global distributions of these gases is a prerequisite to fully understand their role in atmospheric chemistry.

Global distributions of CH_4 and CO are also measured by the MOPITT instrument on board the EOS-TERRA satellite in the near- and thermal infrared (e.g. Drummond and Mand, 1996; Deeter et al., 2003). Up till now, MOPITT has been unsuccessful in retrieving accurate CH_4 total columns from their data. Methane has been measured earlier by the Interferometric Monitoring of Greenhouse Gases (IMG) instrument on board the ADEOS satellite (Clerbaux et al., 1998). Recently, the EOS-AURA satellite was launched, carrying the Tropospheric Emission Spectrometer (TES) instrument, which is currently measuring CH_4 and CO (e.g. Beer et al., 2001). However, retrieved total column products from this instrument are not yet available. Ground-based measurements of CO and CH_4 total columns are available from a number of ground stations, but they do not provide global coverage and a significant fraction of these are at elevated locations. Thus, these stations only measure the total column directly above the station, whereas the larger spatial coverage of a SCIAMACHY ground pixel will mostly also include contributions from lower (polluted) altitudes, where most of the CO and CH_4 resides (de Mazière et al., 2004, Dils et al., 2005[2]).

The retrievals of CO and CH_4 from SCIAMACHY's near-infrared channel 8 have proven more complex than anticipated, due to the presence of an unexpected ice layer on the detectors, which varies in time. Its effects have been reduced by applying dedicated in-flight decontamination procedures and additional in-flight calibration measurements, as well as improvements to the calibration. However, the quantitative effects of these problems on the retrieved CH_4 and CO total columns have only been investigated for very few cases.

This paper focuses on a more systematic investigation of some of the major calibration problems concerning SCIAMACHY's near-infrared channel 8 and the effects of

[2]Dils, B., de Mazière, M., Blumenstock, T., et al.: Comparisons between SCIAMACHY and ground-based FTIR data for total columns of CO, CH_4, CO_2, and N_2O, Atmos. Chem. Phys. Discuss., submitted, 2005.

these problems on the retrieved CH_4 and CO total columns from this channel. The problems addressed in this paper are at present not or insufficiently corrected for in the operational SCIAMACHY data provided by ESA/DLR.

Different corrections for these issues have been developed independently by a number of research groups (e.g. Buchwitz et al., 2004b; Frankenberg et al., 2005; Gloudemans et al., 2004), but the detailed information describing the applied corrections and their impact is often lacking.

In order to determine e.g. CH_4 sources and sinks, and estimate CO emissions from SCIAMACHY measurements, an accuracy of ∼1–2% for CH_4 and ∼10–20% for CO is required. This paper shows that in order to retrieve total columns with those accuracies from channel 8, detailed corrections for all known instrument calibration problems are required. Section 2 discusses the major instrument calibration problems, Sect. 3 describes the retrieval algorithm used, and Sect. 4 shows the retrieval results using SCIAMACHY measurements. The effects of the instrument calibration improvements on the retrieved CH_4 and CO total columns are presented in Sect. 5 as well as comparisons of retrievals in different spectral windows of SCIAMACHY's channel 8. Finally, Sect. 6 discusses all results and the conclusions are summarized in Sect. 7.

2. Instrument calibration

The near-infrared nadir spectra measured by SCIAMACHY's channel 8 (2265 to 2380 nm) contain absorption lines of CH_4, CO, H_2O, and N_2O. However, the retrieval of these species in this wavelength range is complicated due to the low atmospheric signal compared to the instrument dark signal itself (Fig. 1). This dark signal is the sum of the detector dark signal and the thermal background of the instrument and represents the total measured signal when no light is falling onto the instrument itself. SCIAMACHY measurements show that in case of a strong atmospheric signal, corresponding to a surface albedo of 0.55, the dark signal contribution varies from ∼45% at the short wavelength end of channel 8 to ∼75% at the long wavelength end. In the

case of a lower surface albedo, the corresponding lower atmospheric signal results in an even higher contribution of the dark signal as is shown in Fig. 1. Thus, an accurate instrument calibration (dark signal etc.) is required in order to retrieve meaningful total columns from SCIAMACHY's channel 8.

Unfortunately, the retrieval within this wavelength range is hampered by a number of instrument-calibration problems. The most important complication in channel 8 is the growth of an ice layer on the detector. This ice layer is due to spurious water absorbed in the ENVISAT satellite frame. Over time, this water evaporates and most of it escapes to space. However, a small portion is trapped by the SCIAMACHY instrument isolation blankets and freezes out onto the near-infrared detectors. The ice layer increases slowly in time up to a thickness of ~400 μm and leads to losses in the total measured signal of up to ~50%. This loss in signal is partially alleviated by heating the detector every 3–6 months, hereby evaporating the ice layer. However, the decrease of the signal behaves differently after each of these decontamination periods (see Fig. 2 and http://atmos.af.op.dlr.de/projects/scops/ or http://www.sron.nl/~SCIA_CAL/SCIACALtransmission.html). The consequences of the growing ice layer are threefold:

- The signal-to-noise ratio of the spectra is reduced.
- The instrument thermal background contribution to the total dark signal decreases, as the ice layer also absorbs these photons. In order to deal with this, the total dark signal has been measured every orbit, since October 2002 (Kleipool, 2003a).
- Scattering of light in the ice layer gives rise to extended wings in the slit function.

The latter has a significant effect on the retrieved columns and is the most difficult to correct for, since it varies in time and cannot be determined independently. One possibility to determine this broadening of the slit function is by using the in-flight measurements from SCIAMACHY's Spectral Light Source (SLS). However, this spectral

lamp does not illuminate the whole slit and the overlapping line wings in the SLS spectra complicate the use of these measurements to correct for the broadening of the slit function. In addition, the ice layer is not uniform over the whole channel, so that defining a correction method which is applicable at all wavelengths within channel 8 is complicated. Therefore, a different approach has been adopted in the retrievals presented here, which is described in Sect. 3.

Furthermore, the instrument thermal background and thus the total dark signal also varies within an orbit. This is due to the optical bench heating up on the day side of the orbit. The dark signal is measured upon entering the eclipse near the South Pole, where the contribution of the thermal background signal is largest. This ultimately leads to total columns that are too high, especially at high Northern latitudes where the actual dark signal deviates most from the measured dark signal (Kleipool, 2004a). The deviation from the measured dark signal varies over the months, since the dark signal is influenced by the thickness of the ice layer.

Lastly, the near-infrared wavelength range in channel 8 is sampled by 1024 detector pixels, a significant fraction of which have turned “dead” or “bad” during the life time of SCIAMACHY (Kleipool, 2004b). A pixel is labelled “dead” when there is no spectral response and “bad” when the spectral response is too noisy or unpredictable. Since neither “dead” nor “bad” detector pixels should be used in the retrievals, both will be referred to as “dead” pixels throughout this paper for simplicity. The most likely causes for this failure of detector pixels are the manufacturing process itself and in-flight radiation damage (Kleipool et al., 2005, in preparation). The most worrying consequence of this is that the number of dead pixels appears to be increasing steadily in time, at a rate of ∼60 pixels per year. This calls for a time-dependent dead pixel mask to be used in the retrieval codes when retrieving total columns from channel 8. In Sect. 5.3 it will be shown that using one dead pixel in the retrieval code, can lead to erroneous results (see also Kleipool, 2004b).

3. Retrieval algorithm

The retrieval method used here is based on an Iterative Maximum Likelihood Method (IMLM) and has been developed at SRON. The retrieval uses a fixed set of climatological atmospheric profiles based on the US standard atmosphere (1976) to compute a model spectrum in terms of optical depths. For each SCIAMACHY ground pixel these profiles are truncated at the mean surface elevation of the pixel.

Once the optical depths are calculated, the earth radiance can be computed in a forward model (Schrijver, 1999, Gloudemans et al., 2005, in preparation), which is then transformed by an instrument model to represent the radiation detected by the instrument detectors. This modelled spectrum is then fitted – by adjusting the total columns of the different species - to the measured (detector) spectrum in an iterative way. The instrument model also provides an estimate of the instrument noise, from which, by standard statistical methods, an estimate is computed of the instrument-noise related errors in the total columns. A more detailed description of the retrieval algorithm can be found in Schrijver (1999) and Gloudemans et al. (2005, in preparation).

The instrument model used in the current retrievals includes a dedicated time-dependent dead pixel mask, as well as dark signals for every orbit, both of which are taken from the SRON database set up by Kleipool (Kleipool, 2003a, 2004b). A correction for the variation of the dark signal within an orbit is also included (Kleipool, 2004a), as well as a first approximate correction for the broadening of the slit function due to the growing ice layer. The effect of the slit function's extended wings on the spectrum resembles an additional background signal. Therefore, this latter correction involves adding a constant baseline per orbit to the modelled detector spectrum (i.e. independent of wavelength). Since only a small spectral window of channel 8 is used in the retrievals presented here, this appears to be an acceptable approximation, as can also be shown by computing synthetic spectra. The size of the additional background signal has been determined by fixing the SCIAMACHY CH_4 values to the CH_4 total columns over the central part of the Sahara, as calculated by atmospheric chemistry

models. These models show little variation in the CH_4 total columns in space and time over this part of the Sahara and therefore it appears a good region for calibrating the SCIAMACHY data.

All above correction methods, except for the correction for the broadening of the slit function's wings, are the same as those included in the SRON patched level 1 files. It is still under investigation how these correction methods can be refined, but further improvements are expected to be small compared to the effects shown in Sect. 5. In addition, a number of improvements to the retrieval approach are foreseen. For example, only a fixed atmospheric temperature profile has been used at present, but at the time of writing the inclusion of an ECMWF temperature profile in the IMLM retrieval algorithm is being implemented. Although the lack of a correct temperature profile can lead to CH_4 columns that are off by $\lesssim$2% (Gloudemans et al., 2005, in preparation), it will be shown that the problems addressed here have a larger impact on the retrieved columns. Scattering in the atmosphere is not included in the forward model, but is expected to introduce only small corrections (Buchwitz and Burrows, 2004). The retrieved CH_4 and CO total column data presented in this paper have been cloud masked and thus contain only cloud-free measurements. For this, a cloud mask based on the SCIAMACHY Polarisation Measurement Devices (PMDs) 2, 3, and 4 has been included in the IMLM algorithm. This cloud algorithm is similar to that described by Krijger et al. (2005), except that the distinction between ice/snow covered surfaces is not included. The cloud mask by Krijger et al. (2005) is being implemented at the time of writing.

4. Retrieval results

Near-infrared CH_4 and CO total columns from SCIAMACHY have also been reported by others (e.g. Buchwitz et al., 2004a,b; Frankenberg et al., 2004). Qualitative comparisons have shown that the IMLM results agree well with these other data products (e.g. Gloudemans et al., 2004), even though there are significant differences between the algorithms used and the applied instrument calibration.

In order to investigate the effects of the different instrument calibration problems mentioned in Sect. 2 on the retrieved CH_4 and CO total columns, six months of SCIAMACHY channel 8 data have been analysed. The period September 2003 – February 2004 has been chosen, because the available data result in a good global coverage. The start of this period is right after the August 2003 decontamination (duration: 375 h) and also includes the decontamination period in December 2003/January 2004 (duration 338 h), allowing the investigation of instrument-calibration effects after two different decontamination procedures. Results are shown for retrievals in the channel 8 spectral window between 2321–2334 nm. This window is similar to that used by Frankenberg et al. (2004). Results for two other spectral windows of channel 8 are discussed in Sect. 5.4. The data presented in this section include corrections for all instrument-calibration problems mentioned in Sect. 2. Section 5 illustrates in more detail the effects on the retrieval of not including these corrections.

4.1. CH_4

Figure 3 shows the monthly-averaged CH_4 results for November 2003. Only cloud-free ground pixels with a high enough signal-to-noise ratio have been included in the SCIAMACHY retrievals. The lack of data over the oceans is due to the fact that the surface albedo is too low, resulting in a signal-to-noise ratio which is too small to perform accurate retrievals. At high latitudes ($\gtrsim 70^\circ$ N) the signal-to-noise ratio is also too low.

Unfortunately, no independent satellite-based CH_4 total column measurements are available, so that the SCIAMACHY CH_4 total columns can only be compared to total columns from ground-based stations or calculations from atmospheric chemistry transport models. Comparisons of the IMLM total columns with ground-based measurements are presented by Dils et al. (2005)[3], but these do not provide global coverage.

[3]Dils, B., de Mazière, M., Blumenstock, T., et al.: Comparisons between SCIAMACHY and ground-based FTIR data for total columns of CO, CH_4, CO_2, and N_2O, Atmos. Chem. Phys. Discuss., submitted, 2005.

Therefore in Fig. 3, the retrieved CH_4 total columns are compared with calculations by the chemistry transport model TM3 from the Royal Netherlands Meteorological Institute (KNMI). A detailed description of the TM3 model used here can be found in Dentener et al. (2003) and references therein. The model includes CH_4 emissions closely following Houweling et al. (1999). These model calculations show a good agreement with in situ measurements (http://www.cmdl.noaa.gov/ccg/) and reproduce the background CH_4 levels well. Although most chemistry transport models do not contain up-to-date emissions and the model resolution is mostly coarser than the resolution of the SCIAMACHY ground pixels (e.g. 2° by 3° as opposed to 120×30 km, i.e. ∼1.1° by 0.27° at the equator) they do provide accurate information on the large scale distribution of CH_4, such as the North-South gradient and well-known continuous or seasonal sources and sinks.

Figure 3 shows that such a qualitative comparison shows good agreement between the monthly-averaged SCIAMACHY data and the corresponding TM3 calculations. For instance, the North-South gradient is clearly visible in the SCIAMACHY data. In addition, many differences can be identified as well, such as the polluted areas in Eastern USA, and the East coast of Australia, which are hardly visible in the TM3 model. The origin of these differences is still under investigation. In Central Africa between ∼10° S and ∼5° N a region with low CH_4 columns is visible which is not in agreement with the TM3 calculations. Since this region is mostly cloudy during this time of the year, this is probably due to cloudy SCIAMACHY ground pixels that have not been filtered out by the cloud mask included in the IMLM retrieval algorithm. Other persistently cloudy areas such as in the Amazon basin are also clearly identified by the lack of SCIAMACHY data. In addition, low CH_4 columns are seen in West Africa between ∼5–15° N. This area is known for the presence of forest fires and the corresponding smoke may not be picked up by the cloud mask. Smoke and/or clouds shield the CH_4 in the lower parts of the atmosphere, resulting in too low CH_4 total columns measured by SCIAMACHY. Retrieval of CO_2, another well-mixed gas, from SCIAMACHY's channel 6, also results in too low total columns of a few percent in the same area, using the same cloud mask

(W. Hartmann, SRON, private communication).

Figure 4 shows a more quantitative comparison of the monthly-averaged CH_4 total columns from the IMLM retrieval algorithm with TM3 for September 2003. Here, the globe has been divided in five-degree latitude bins. All SCIAMACHY data within each latitude bin have been averaged over the whole month and compared to the monthly average of the collocated TM3 CH_4 total columns within the same latitude bin. Both data sets have been normalized to surface pressure prior to averaging. The results show a good agreement between latitudes 40° S and 5° S and on the Northern Hemisphere ($\gtrsim$15° N). In both regions the difference between the retrieved CH_4 columns and the TM3 calculations is less than ~2%, except for the region North of 65° N, where it is ~5%. This region may suffer from higher solar zenith angles or cloudy ground pixels, resulting in erroneous CH_4 columns. The area between 5° S and 15° N is mostly cloudy at this time of the year, as is also seen for November 2003 in Fig. 3, and may also be affected by smoke from the forest fires, resulting in lower CH_4 total columns and less collocations with TM3.

Although only comparisons for two months, September and November 2003, are shown here, the other months do give similar results (see also Straume et al., 2005).

4.2. CO

Independent satellite-based CO total column measurements are available, unlike for CH_4. Especially for CO, which has strong temporal and spatial variations, such satellite intercomparisons provide a very valuable validation technique. The MOPITT instrument is currently the only other instrument from which CO total column measurements from space are available. MOPITT uses gas-correlation spectroscopy, based on pressurized cells (Drummond and Mand, 1996), whereas SCIAMACHY uses a grating spectrometer. In addition, SCIAMACHY measures CO in the near-infrared, while MOPITT observes CO in the thermal infrared, where the CO lines are much stronger than in the near-infrared. Thus, measurements from these satellites provide two independent sets of CO total column products, making them very suitable for a first qualitative

comparison with the retrieved SCIAMACHY CO total columns. In the near-infrared, the surface reflectance over the oceans is very low, complicating the SCIAMACHY retrievals in these areas. Measurements in the thermal infrared however have a lower sensitivity to the boundary layer, due to small temperature contrasts with respect to the surface. In those cases, a priori information is added to the MOPITT CO measurements. Since this is more likely to happen at night, only day-time MOPITT measurements are taken into account.

Monthly-averaged results for CO compared with measurements by the MOPITT instrument are shown in Figs. 5 and 6 for November and September 2003. Only cloud-free ground pixels with a high enough signal-to-noise ratio have been included in the SCIAMACHY retrievals shown here.

The SCIAMACHY CO total columns for November 2003 shown in Fig. 5 are in good agreement with the MOPITT measurements of that month. The data sets show a good agreement on both the Northern and Southern Hemisphere, and enhanced CO columns in West and Central Africa and Brazil due to bio-mass burning. Similar enhanced CO columns are reported by Frankenberg et al. (2004), using the same SCIAMACHY data, but using a different retrieval algorithm (Frankenberg et al., 2005). This is the same region where the low CH_4 columns are seen in Fig. 3, providing further evidence for the low CH_4 columns being due to smoke from forest fires (see Sect. 4.1).

Well-known polluted areas, such as in Asia, are also clearly visible in Fig. 5 as regions with enhanced CO total columns. Mountainous areas, such as the Himalayas and the Andes, show up in both the SCIAMACHY and MOPITT measurements as regions with low CO total columns. Large differences are also observed: the forest fires are more pronounced in the SCIAMACHY data than in the MOPITT measurements, and the retrieved SCIAMACHY total columns also show higher CO values over India and Eastern USA. Part of this difference may come from the fact that the MOPITT measurements are less sensitive to the boundary layer resulting in lower CO total columns (Deeter et al., 2003). In this comparison, the difference in the averaging kernels for the MOPITT and SCIAMACHY instrument has not been taken into account. A more

detailed comparison of these two sets of satellite measurements is currently planned in close collaboration with the National Center for Atmospheric Research (NCAR).

A somewhat more quantitative comparison of the IMLM CO total columns with MOPITT is shown in Fig. 6. This figure is constructed in a similar way as Fig. 4 for CH_4. It can be seen that there is a good agreement between the two data sets for September 2003. Differences are generally within 10%, except for the region between ~0° and ~15° N where the differences are up to ~20%. This may be due to the relatively few data points in this area, due to clouds.

As is the case for CH_4, the other months in the period September 2003–February 2004 show similar CO SCIAMACHY–MOPITT comparisons (see also Straume et al., 2005). For January 2004, the quality of the retrieved CO columns cannot be derived from comparisons with MOPITT data, since only a few days of MOPITT data are available for this month.

5. Effects of instrument calibration on the retrieved total columns

5.1. Effects of the growing ice layer

The effect of the broadening of the slit function due to ice growth on SCIAMACHY's channel 8 detector has been investigated by performing retrievals with and without a correction for the slit function. The resulting CH_4 and CO total columns are shown on a daily basis in Fig. 7, since the thickness of the ice layer varies strongly in time. In order to avoid influences of other time-dependent events, such as seasonal variation of CH_4 sources and sinks or polluted areas, only the retrieved total columns over the Sahara are taken into account, since the CH_4 and CO variation due to atmospheric processes is expected to be low in this region (Houweling et al., 1999). Figure 7a shows the results for CH_4, where, for each day, the CH_4 total columns are normalized to the mean surface elevation of the corresponding SCIAMACHY pixel and then averaged over the Sahara. Note that this is a larger area than that used to determine the correction for

the slit function (see Sect. 3). The difference between retrievals with and without slit-function correction is clearly visible. The CH_4 total columns retrieved with a correction for the slit function show an almost constant behaviour in time, in good agreement with calculations by the TM3 model. The trend in the CH_4 total columns for retrievals without slit-function correction resembles the loss in the measured total signal for this period, corresponding to the growth of the ice layer (see Fig. 2). The differences between retrievals with and without correction for the slit function range from ~6% shortly after a decontamination to 17.5% four months later, in December 2003.

Figure 7b shows the results for the retrieved CO total columns. A strong correlation with the loss in the measured total signal due to the growing ice layer, as is present for CH_4, cannot be seen for CO, but Fig. 7c shows the difference between the CO total columns retrieved without and with correction for the slit function respectively, relative to the CO total columns with slit-function correction. It can be seen that the relative difference correlates well with the loss in the total signal, indicating that the retrieved CO total columns are also clearly affected by the broadening of the slit function due to the growing ice layer. Differences between retrieved CO total columns with and without correction for the slit function range from ~10% shortly after a decontamination to ~35% four months later in December 2003. While the differences for CH_4 are significantly larger than the current accuracy of the retrieved CH_4 total columns of a few %, the differences for CO are comparable to the current accuracy of the retrieved CO total columns (cf. Dils et al., 2005[4]; Straume et al., 2005). However, the clear trend in Fig. 7c strongly suggests that the precision of the CO retrievals is much better than the current CO accuracy. Thus, although the correction for the slit function may seem less important for CO than for CH_4, the CO total columns are still significantly affected by the ice layer.

[4]Dils, B., de Mazière, M., Blumenstock, T., et al.: Comparisons between SCIAMACHY and ground-based FTIR data for total columns of CO, CH_4, CO_2, and N_2O, Atmos. Chem. Phys. Discuss., submitted, 2005.

5.2. Effects of the dark signal orbital variation

Although the orbital variation of the dark signal is much smaller than the slit-function correction, it does have an effect on the retrieved columns, especially at Northern latitudes where the deviation of the actual dark signal from the measured dark signal reaches its largest values (Sect. 2). The effect of the variation of the dark signal over the orbit has been tested by performing retrievals with and without a correction for the orbital variation. This correction is taken from the data base set up by Kleipool (Kleipool, 2004a). To demonstrate the effect of the orbital variation on the retrieved columns, monthly-averaged data have been investigated for the period September 2003–February 2004. Only the region between longitudes 30° W and 60° E has been investigated, since it has a good data coverage and large regions with high signal-to-noise ratio.

Since both the retrievals with and without correction for the orbital variation do include a correction for the slit function, which is much larger than the orbital variation itself, the two data sets should in principle not show a time-dependent behaviour due to the ice growth. This is true for the retrieved total columns including the correction for the orbital variation, which is done on an orbital basis. However, some time dependency is expected for the retrieved total columns without the correction for the orbital variation. Firstly, the orbital variation is linearly dependent on the measured signal, which decreases in time due to the ice growth. Secondly, the orbital variation is defined as a function of orbit phase, with orbit phase 0 corresponding to the start of the night side. Since phase 0 changes seasonally, this is expected to cause small time-dependent behaviour in the retrieved total columns without a correction for the orbital variation as a function of latitude. Therefore also the differences between the two data sets are expected to show some small time-dependent behaviour.

Figure 8a shows the relative differences between the monthly averaged CH_4 total columns without and with correction for the orbital variation respectively, in percentages of the retrievals with this correction. The results are shown as a function of latitude,

where data within 5 degree latitude bins have been averaged prior to determining the differences. A clear increase in the relative difference can be seen towards Northern latitudes for all months, as expected. The difference is $\gtrsim$2% for latitudes $\gtrsim$45° N, and increases to ~4–5% at high Northern latitudes. This is a significant effect, since Fig. 4 showed typical differences between retrieved CH_4 and TM3 calculations of $\lesssim$2% outside the region between ~5° S and ~15° N (see Sect. 4.1). Similar values for the accuracy of the CH_4 total columns are reported by Gloudemans et al. (2004) and Dils et al. (2005)[5].

The bump between ~15° S and ~10° N correlates well with the change in reflectance in this latitude range. Lower reflectances correspond to a lower signal level, resulting in a larger relative effect of the orbital variation, whereas higher signal levels result in a smaller effect. However, Fig. 8 shows that variations in the reflectance do not cause relative differences of more than ~1%, which is much lower than the differences seen above ~45° N. This strengthens the conclusion that the increase in the relative differences at high Northern latitudes are due to the increase in the dark signal over the orbit. Some differences between the different months are visible, but these are smaller than or comparable to the current accuracy of the CH_4 retrievals and are likely due to a combination of ice growth in time and the seasonal variation of the time of eclipse.

For CO, the effect of the orbital variation of the dark signal is not as evident as for CH_4. In Fig. 8b, a decrease in the relative difference of the CO total columns without and with a correction for the orbital variation, can be seen towards higher latitudes for all months. However, the differences are generally within 15%, corresponding to the accuracy of the monthly-averaged retrieved CO total columns (Sect. 4.2 and Table 1). The apparent trend in the relative differences for CO is opposite to that for CH_4 (Fig. 8). This is probably due to the many CH_4 lines in channel 8, which are often (partially) overlapping with the much weaker and scarcer CO lines. This requires the CO lines

[5]Dils, B., de Mazière, M., Blumenstock, T., et al.: Comparisons between SCIAMACHY and ground-based FTIR data for total columns of CO, CH_4, CO_2, and N_2O, Atmos. Chem. Phys. Discuss., submitted, 2005.

to be fitted simultaneously with the CH_4 lines, indicating that the retrieved CO total columns may be influenced by the fit to the CH_4 lines in a non-linear way. Higher CH_4 total columns may fill in part of the CO absorption lines, leading to lower retrieved CO total columns, but lower CH_4 total columns do not necessarily result in higher retrieved CO total columns as e.g. can be seen in Sect. 5.1. Although the effect of the orbital variation does not exceed the current accuracy of the retrieved CO total columns, the clear trend seen for all six months strongly suggests that the precision of the CO retrievals is much better, as is also indicated by the slit-function effect in Sect. 5.1 and Fig. 7. Thus, it is important to also correct the CO total columns for the orbital variation.

5.3. Effects of the dead pixels

The previous sections show that both the orbital variation and the growth of the ice layer result in a systematic, time-dependent effect on the retrieved columns. The dead detector pixels in SCIAMACHY's channel 8 are not expected to result in systematic effects. Although the number of dead pixels increases in time due to radiation damage (Kleipool et al., 2005, in preparation), the effect of dead pixels does not depend on their total number but on their spectral location. A pixel that does not sample (part of) an absorption line, is not expected to have an effect on the retrieved total columns, whereas a pixel that lies at the centre of an absorption line is much more likely to affect the retrievals.

In the case of CO, only a few absorption lines are present in the wavelength range of channel 8. These lines are most of the time barely above the noise level, many times weaker than the (often overlapping) CH_4 lines in the same spectra. Thus, even without dead pixels, retrieval of CO total columns from SCIAMACHY spectra is difficult. The presence of dead pixels and the corresponding loss of spectral information further complicates the CO retrievals. Unfortunately, a significant number of dead pixels are already located at or near the centre of CO lines. Therefore, there is a realistic possibility that an insufficient number of good detector pixels is left to retrieve accurate CO

total columns well before the end of SCIAMACHY's life time.

On the other hand, the wealth of strong CH_4 lines in the wavelength range of SCIAMACHY's channel 8, ensures that the CH_4 retrievals are not easily influenced by dead pixels, as long as the dead pixels are not used when fitting the SCIAMACHY spectrum. However, Fig. 9 shows that the CH_4 retrievals are affected significantly, when this is not done correctly.

Thus, in order to perform accurate CO and CH_4 retrievals, a good identification of the dead pixels is required. There are two complications in deriving such a dead pixel mask. The first is the fact that detector pixels are damaged by radiation, mostly resulting in an abrupt change in their dark signal. Although detection of such dead pixels is relatively easy, it results in a slow but almost constant increase of dead pixels over time.

The second problem is that a significant number of bad detector pixels in channel 8 show regular jumps between two or more discrete levels of the dark current on timescales varying from less than ~1 second to several days or longer. This implies that for some pixels the dark current during the SCIAMACHY measurement on the day side may be significantly different from the reference dark current measured at the night side. The size of these jumps can vary from values comparable to the noise in the dark current measurements to values comparable to the dark current itself. These so-called Random Telegraph Signal (hereafter: RTS) pixels can only be detected if the dead pixel identification algorithm includes a statistical constraint.

In order to deal with this, an algorithm has been developed that derives a dead pixel mask from the instrument calibration data for each orbit, which includes the physical characteristics of the detector pixels such as the dark signal. Then, a statistical method is used to filter out noise and to detect the so-called RTS pixels by including the information from the last 50 orbits, corresponding to ~3.5 days. This will ensure that radiation-damaged pixels as well as RTS pixels are detected quickly and accurately.

The dead pixel mask used in the current retrievals only masks a pixel if its physical characteristics are bad for more than 25% of this period. This mask has been tested

and works well: analyzing retrievals for a whole year, only a few dead pixels have been found that are not masked. For each of these pixels, this is only the case for a period of ~1 day, after which each of them is masked correctly. Putting stronger constraints on the physical characteristics leads to a significantly larger number of dead pixels, including pixels that are still performing reasonably, further complicating the retrievals in channel 8. Therefore, it occasionally happens that a dead pixel does not appear in the pixel mask instantly, but only after ~1 day. The current dead pixel mask is still being checked regularly and the current constraints may have to be adapted over time, to maintain a good performance.

However, even missing one pixel in the dead pixel mask for such a short period can have a significant effect on the retrievals. An example of this effect is shown for one such pixel, which is dead based on its physical quantities, but does not show up in the dead pixel mask until after ~0.85 day or equivalently, 12 SCIAMACHY orbits. This pixel is located at the position of a CH_4 line, but not near a CO line. Fig. 10 shows the results for retrievals with and without masking this dead pixel during its ~0.85 day period in February 2004, and then averaging all retrieved CH_4 and CO total columns for that whole month. Comparing retrievals with and without masking this pixel clearly shows that it creates artificially low CH_4 columns in some areas, but it may not be that obvious that something is wrong from Fig. 10b only. Similarly, looking at Fig. 10d only, may lead to the conclusion that enhanced CO emission is seen over Iraq.

In this case, the retrievals of the individual orbits clearly indicate that something is wrong, by means of the large fit residuals. In fact, most of the time the few dead pixels that are missed are easily identified, since they cause large fit residuals and unrealistic values for the retrieved CH_4 and/or CO total columns. However, a few cases have been found where a pixel with truly bad physical characteristics still gives good fit residuals. Investigation of the effect of one such dead pixel, leads to similar results as seen in Fig. 10: enhanced CO emission is seen over India, which disappears when this pixel is masked out. In the unlikely case that such a pixel is missed by the dead pixel mask, a good way to detect such dead pixels is by comparing retrievals from different

wavelength ranges (see Sect. 5.4).

These results indicate that the identification of dead pixels is best done by monitoring their physical behaviour, but inspecting the retrievals afterwards for strange anomalies remains important. Identification of dead pixels by means of fit residuals only appears insufficient and may lead to misinterpretation of the results.

5.4. Effect of retrieval windows

The results presented in the previous sections are based on retrievals in a single spectral window of SCIAMACHY's channel 8 between 2321–2334 nm (hereafter: window 1). Since this is not the only part of channel 8 that contains CO and/or CH_4 absorption lines, two other spectral windows, containing both CH_4 and CO lines, have been investigated. The results for all three windows are summarized in Table 1.

Window 2 covers the range 2327–2339 nm, and is chosen for the presence of strong CO lines that are relatively unaffected by the dead pixels. It overlaps partially with window 1 which has been used so far and thus similar results are expected. Indeed, the retrieved CH_4 total columns are very similar to those from window 1, with monthly-averaged CH_4 results also differing from TM3 calculations by $\lesssim$2%. Comparisons of monthly-averaged CO results with MOPITT measurements show a good agreement between the two data sets, with differences within ~15%.

The differences between retrievals with and without correction for the slit function vary between ~8% and ~19.5% for CH_4 and between ~15% and ~46% for CO. This may suggest a slightly thicker ice layer in this wavelength range compared to window 1.

The effect of the orbital variation of the dark signal is also similar to that in window 1, i.e. relative differences of up to ~4–5% for CH_4 and up to ~15% for CO at high Northern latitudes.

Window 3 ranges from 2354–2370 nm. This window is similar to the spectral range used by Buchwitz et al. (2004a) and contains CO lines from the *P*-branch, whereas the

other windows contain R-branch CO lines. The monthly-averaged CH_4 total columns compare well with TM3 calculations and with results from the other two windows, although the differences with TM3 of $\lesssim$3% on the Southern Hemisphere are slightly larger than for window 1 and 2, and the deviation from TM3 seems to increase somewhat for high Northern latitudes. Comparisons of monthly-averaged CO results with MOPITT measurements result in deviations of ~30%, larger than for the other two windows. Here, the retrieved CO total columns are mostly lower than those from MOPITT, whereas window 1 shows total columns somewhat larger and window 2 somewhat lower than MOPITT.

The effect of the broadening of the slit function due to the growing ice layer ranges from ~6% to ~18% for CH_4 in window 3, comparable to that of the other two windows. Although the atmospheric signal in this wavelength range is lower than in the other two windows, the slit-function broadening causes a relative effect on the CH_4 total column, thus explaining the similarity with the other two windows. For CO the difference between retrievals with and without correction for the slit function shows no clear trend in time and ranges from ~2% at the beginning of September 2003 to ~25% around mid December, to ~20% in early January just after the decontamination. This is probably related to the dead pixels in window 3, resulting in few CO lines that are unaffected. One particular pixel, which lies at the center of a strong CO line, causes the retrieval algorithm to give a wrong fit to the remaining detector pixels containing parts of the other CO lines. This probably explains the low retrieved CO total columns for window 3.

The effect of the orbital variation of the dark signal in window 3 is larger than in the other windows and can be up to ~13% for CH_4 at high Northern latitudes. For CO, the effect is also larger than in the other windows, up to ~30%, increasing towards Northern latitudes, whereas it is decreasing for the other windows. As for the other windows, the relative difference for CO is comparable to the accuracy of the CO total columns, making the effect of the orbital variation less pronounced for CO than for CH_4. The larger effect of the orbital variation and the increasing differences for CO are probably

due to the lower atmospheric signal in this wavelength range compared to the other windows (see Fig. 1). The lower signal introduces a larger effect on the retrieved total columns from window 3 for calibration issues with wavelength independent behaviour. The absolute values of the orbital variation of the dark signal show only a weak dependency on wavelength, thus explaining the larger relative differences in window 3. The lower atmospheric signal in window 3 also requires a better calibration, and thus the retrieved CH_4 and CO total columns may suffer from larger uncertainties. In addition, the dead pixels may play a role for CO in this window.

The number of dead pixels in all three windows are comparable, but it depends on the spectral location of these pixels whether the retrievals in one window give better results than in the other. The good agreement of the retrieved CH_4 total columns in all three windows gives some indication that in terms of dead pixels no window is preferred over another for the considered time period, and that no dead pixels that are important for the CH_4 retrievals are missed by the dead pixel mask. For CO, it seems that window 3 is preferred less than window 1 and 2, but using only part of window 3 results in CO total columns that are more in agreement with the results from the other two windows. Thus, using different windows in SCIAMACHY's channel 8 seems a good way to verify the retrieved CH_4 and CO total columns and thus improve their accuracy.

6. Discussion

The previous sections show that the growing ice layer, the orbital variation of the dark signal, and the dead pixels can cause significant errors in the retrieved CH_4 and CO total columns, when no or inaccurate corrections are taken into account. The nature of each of these effects is different. Whereas the effect of the growing ice layer varies strongly on the order of days, the effect of the orbital variation of the dark signal shows almost no time dependency. Also, both the growing ice layer and the orbital variation cause systematic effects in the retrieved CH_4 and CO total columns, whereas the effect of the dead pixels is a random one. Applying accurate corrections for these instrument

calibration problems significantly improves the retrieved CH_4 and CO total columns.

Although the instrument calibration problems discussed in this paper have the largest impact on the retrieved total columns in SCIAMACHY's channel 8, additional smaller problems exist. As mentioned in Sect. 2, the dark signal decreases in time due to the growing ice layer and is currently measured for every SCIAMACHY orbit. However, the dark signal measurements are not available for every orbit for which SCIAMACHY data is present, due to incomplete data distribution and different versions of the distributed data. This may lead to small inaccuracies in the retrieved total columns, especially right after decontamination, when the dark signal is dropping fastest due to the ice growth. These are not expected to be larger than a few percent, which is within the current accuracy of the retrieved CH_4 and CO columns. Another possible error source is the non-linearity as reported by Kleipool (2003b). For channel 8 this effect is small and errors in the retrieved total columns of less than a few percent are expected. A more detailed calculation of these effects will be provided in a future paper. The instrument calibration issues mentioned in this paper apply to both SCIAMACHY's channels 7 and 8. Channel 7 also suffers from an additional serious problem, caused by a light leak.

In Sects. 5.3 and 5.4 it is mentioned that comparison of retrievals in different wavelength ranges gives additional information on the accuracy of the retrieved total columns. Here, only retrievals in SCIAMACHY's channel 8 have been discussed. For CH_4, useful independent information can also be derived from SCIAMACHY's only other near-infrared channel 6, which covers the wavelength range 1000–1750 nm. This channel does not have an ice layer on its detector, and is not hampered by the orbital variation of the dark signal, due to the much higher atmospheric signal in this wavelength range. However, the spectral window containing CH_4 lines contains more dead pixels than in channel 8, non-linearity plays an important role, and scattering in the atmosphere complicates the retrieval. Nevertheless, CH_4 total column retrievals from channel 6 are foreseen for comparison with the CH_4 total columns presented in this paper.

7. Conclusions

In this paper, the effects of three important instrument calibration issues on the retrieved CH_4 and CO total columns from SCIAMACHY's channel 8 are discussed: the broadening of the slit function due to the growing ice layer on the detector, the variation of the dark signal over the orbit, and the dead detector pixels. The main conclusions are as follows:

- The CH_4 and CO total columns retrieved with the IMLM retrieval algorithm, including corrections for all known instrument calibration issues, compare well with calculations from the atmospheric chemistry transport model TM3 and independent measurements from the MOPITT instrument on board the EOS-TERRA satellite.
- The slit-function broadening due to the growing ice layer causes a time-dependent systematic effect on both the CH_4 and CO total columns. For CH_4, this effect is much larger than the precision of ~1–2% required to detect CH_4 sources and sinks. The clear trend seen for CO, corresponds well with the loss in the total signal, indicating that also CO is significantly affected.
- The orbital variation of the dark signal also causes a systematic effect, but has only a small time dependency. This effect is much smaller than the effect of the slit function, but is still significant for both CH_4 and CO, especially at high Northern latitudes.
- The effect of the dead pixels is of a random nature and therefore difficult to quantify in a general sense. An accurate algorithm which identifies the dead pixels for every orbit is required in order to avoid misinterpretation of the retrieved total columns. The dead pixel mask used in the IMLM retrieval is based on the physical characteristics of the detector pixels and works well. Nevertheless, inspecting the fit residual remains important since it provides additional information. However, a dead pixel mask based on fit residuals only is insufficient.

– Retrievals in different wavelength ranges within SCIAMACHY's channel 8 give similar results for CH_4, but show some differences for CO. This is probably due to the scarcity and weakness of the CO lines in combination with the dead pixels, which complicates the CO retrievals significantly.

– Comparison of retrievals in different wavelength ranges provides a useful tool to detect imperfections in the applied instrument calibration corrections and helps to improve the quality of the retrieved total columns.

Acknowledgements. The authors would like to thank the SCIAMACHY and ENVISAT teams who have participated in the planning, building, launching, and operating of the SCIAMACHY instrument. They thank the Netherlands SCIAMACHY Data Center (NL-SCIA-DC) for providing us data and processing services. They also thank Ruud Hoogeveen and Ahilleas Maurellis at SRON for useful discussions. The MOPITT data presented in this paper were obtained from the NASA Langley Research Center Atmospheric Sciences Data Center. The work performed for this publication is (partly) financed by the Netherlands Agency for Aerospace Programmes (NIVR) and the European Commission (Fifth Framework Programme on Energy, Environment, and Sustainable Development, Contract no. EVG-1-CT-2002-00079, project EVERGREEN).

References

Beer, R., Glavich, T. A., and Rider, D. M.: Tropospheric emission spectrometer for the Earth Observing System's Aura satellite, Applied Optics, 40, 2356–2367, 2001. 1735

Buchwitz, M. and Burrows, J. P.: Retrieval of CH_4, CO, and CO_2 total column amounts from SCIAMACHY near-infrared nadir spectra: Retrieval algorithm and first results, in Remote Sensing of Clouds and the Atmosphere VIII, edited by: Schäfer, K. P., Comèron, A., Carleer, M. R., and Picard R. H., Proceedings of SPIE, 5235, 375–388, 2004. 1740

Buchwitz, M., de Beek, R., Bramstedt, K., et al.: Global carbon monoxide as retrieved from SCIAMACHY by WFM-DOAS, Atmos. Chem. Phys., Vol. 4, pp 1945-1960, 2004a 1740, 1752

Buchwitz, M., de Beek, R., Burrows J.P., et al.: Atmospheric methane and carbon dioxide from SCIAMACHY satellite data: initial comparison with chemistry and transport models, Atmos.

Chem. Phys. Discuss., 4, 7217–7279, 2004b,
SRef-ID: 1680-7375/acpd/2004-4-7217. 1736, 1740

Clerbaux, C., Chazette, P., Hadji-Lazaro, J., Mégie, G., Müller, J.-F., and Clough, S. A.: Remote sensing of CO, CH_4, and O_3 using a spaceborne nadir-viewing interferometer, J. Geophys. Res., 103, D15, 18 999–19 013, 1998. 1735

Deeter, M. N., Emmons, L. K., Francis, G. L., et al.: Operational carbon monoxide retrieval algorithm and selected results for the MOPITT instrument, J. Geophys. Res., 108, D14, 4399–4409, 2003. 1735, 1744

de Mazière, M., Barret, B., Blumenstock, T., et al.: Comparisons between SCIAMACHY scientific products and ground-based FTIR data for total columns of CO, CH_4, and N_2O, in Proc. Second Workshop on Atmospheric Chemistry Validation of ENVISAT (ACVE-2), ESA/ESRIN, Frascati, Italy, 3–7 May 2004, (ESA SP-562, August 2004), ESC02MDM, 2004. 1735

Dentener, F., van Weele, M., Krol, M., Houweling, S., and van Velthoven, P.: Trend and interannual variability of methane emissions derived from 1979–1993 global CTM simulations, Atmos. Chem. Phys., 3, 73–88, 2003,
SRef-ID: 1680-7324/acp/2003-3-73. 1742

Drummond, J. R. and Mand, G. S.: The Measurements of Pollution in the Troposphere (MOPITT) Instrument: Overall Performance and Calibration Requirements, Journal of Atmospheric and Oceanic Technology, 13, 314, 1996. 1735, 1743

Frankenberg, C., Platt, U., and Wagner, T.: Retrieval of CO from SCIAMACHY onboard ENVISAT: detection of strongly polluted areas and seasonal patterns in global CO abundances, Atmos. Chem. Phys. Discuss., 4, 8425–8438, 2004,
SRef-ID: 1680-7375/acpd/2004-4-8425. 1740, 1741, 1744

Frankenberg, C., Platt, U., and Wagner, T.: Iterative maximum a posteriori (IMAP)-DOAS for retrieval of strongly absorbing trace gases: Model studies for CH_4 and CO_2 retrieval from near infrared spectra of SCIAMACHY onboard ENVISAT, Atmos. Chem. Phys., 5, 9–22, 2005,
SRef-ID: 1680-7324/acp/2005-5-9. 1736, 1744

Gloudemans, A. M. S., Schrijver, H., Straume, A. G., et al.: CH_4 and CO total columns from SCIAMACHY: Comparisons with TM3 and MOPITT, in Proc. Second Workshop on Atmospheric Chemistry Validation of ENVISAT (ACVE-2), ESA/ESRIN, Frascati, Italy, 3–7 May 2004 (ESA SP-562, August 2004), ESC02AG, 2004. 1736, 1740, 1748

Houweling, S., Kaminski, T., Dentener, F., Lelieveld, J., and Heimann, M.: Inverse modeling of methane sources and sinks using the adjoint of a global transport model, J. Geophys. Res., 104, D21, 26 137–26 160, 1999. 1742, 1745

Kleipool, Q.: SCIAMACHY SODAP: Algorithm Specification for Dark Signal Determination, Tech. Report SRON-SCIA-PhE-RP-009, SRON, 2003a. 1737, 1739

Kleipool, Q.: SCIAMACHY: Recalculation of OPTEC5 Non-Linearity, Tech. Report SRON-SCIA-PhE-RP-013, SRON, 2003b. 1755

Kleipool, Q.: SCIAMACHY: Orbital Variation of dark signal, Tech. Report SRON-SCIA-PhE-RP-18, SRON, 2004a. 1738, 1739, 1747

Kleipool, Q.: SCIAMACHY: Evolution of Dead and Bad Pixel Mask, Tech. Report SRON-SCIA-PhE-RP-21, SRON, 2004b. 1738, 1739, 1769

Krijger, J. M., Aben, I., and Schrijver, H.: Distinction between clouds and ice/snow covered surfaces in the identification of cloud-free observations using SCIAMACHY PMDs, Atmos. Chem. Phys. Discuss., 5, 815–845, 2005, 2005. SRef-ID: 1680-7375/acpd/2005-5-815. 1740

Rodgers, C. D.: Inverse Methods for Atmospheric Sounding, World Scientific, London, 2000.

Schrijver, H.: Retrieval of carbon monoxide, methane and nitrous oxide from SCIAMACHY measurements, in Proc. ESAMS, European Symposium on Atmospheric Measurements from Space, ESA WPP-161 1, ESTEC, Noordwijk, The Netherlands, 285–294, 1999. 1739

Straume, A. G., Schrijver, H., Gloudemans, A. M. S., et al.: The global variation of CH_4 and CO as seen by SCIAMACHY, Adv. Space Res., accepted, 2005. 1743, 1745, 1746

Table 1. Summary of retrieval results in different spectral windows.

#	Window λ (nm)	(IMLM-TM3)/TM3 CH_4[a] (%)	(IMLM-MOPITT)/MOPITT CO[a] (%)	Ice growth effect CH_4[b] (%)	Ice growth effect CO[b] (%)	Effect of Orbital variation CH_4[c] (%)	Effect of Orbital variation CO[c] (%)
1	2321–2334	$\lesssim 2$	<15	6–17.5	10–35	<5	$\lesssim 15$
2	2327–2339	$\lesssim 2$	$\lesssim 15$	8–19.5	15–46	<5	$\lesssim 15$
3	2354–2370	$\lesssim 3$	$\lesssim 30$	6–18	2–25	<13	$\lesssim 30$

[a] For monthly-averaged total columns only. Differences for daily data are somewhat larger.

[b] Based on daily averaged total columns over the Sahara (Sect. 5.1).

[c] Based on monthly-averaged total columns between 30° W and 60° E (Sect. 5.2).

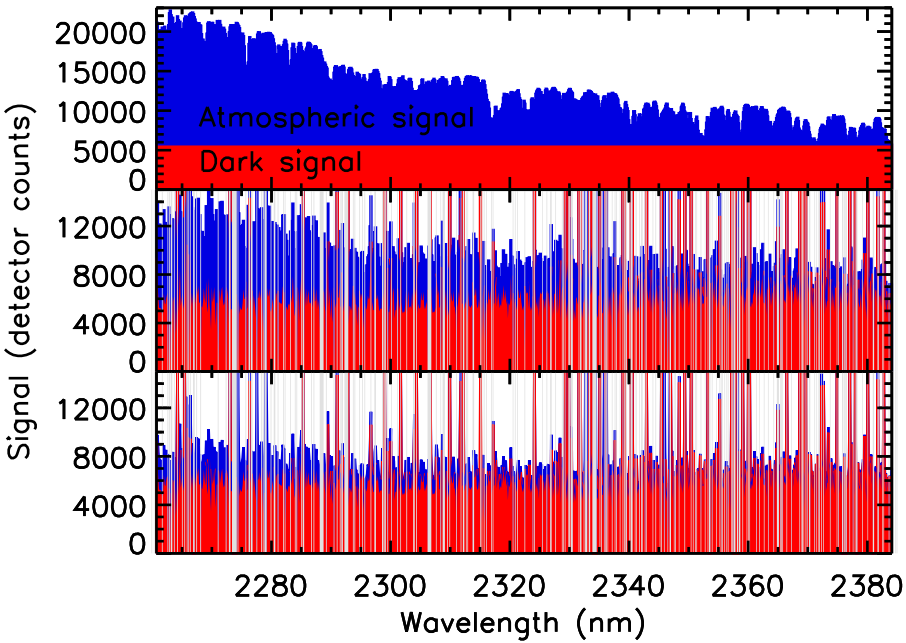

Fig. 1. The total signal, i.e. dark signal + atmospheric signal, as measured by SCIAMACHY's channel 8 detector. The total dark signal is shown in red, the atmospheric signal in blue. The white vertical lines denote the positions of the dead detector pixels at the end of February 2004. Top: Simulated SCIAMACHY measurement in the case of a strong atmospheric signal, assuming a noise-free dark signal. Middle: SCIAMACHY measurement over the Sahara with a high surface albedo of 0.55. The relative contribution of the dark signal of the SCIAMACHY instrument to the total measured signal varies from ~45% at 2260 nm to ~75% at 2380 nm. Bottom: SCIAMACHY measurement over Central Africa with a lower surface albedo of 0.11. The relative contribution of the dark signal of the SCIAMACHY instrument to the total measured signal varies from ~63% at 2260 nm to ~97% at 2380 nm.

ACPD
5, 1733–1770, 2005

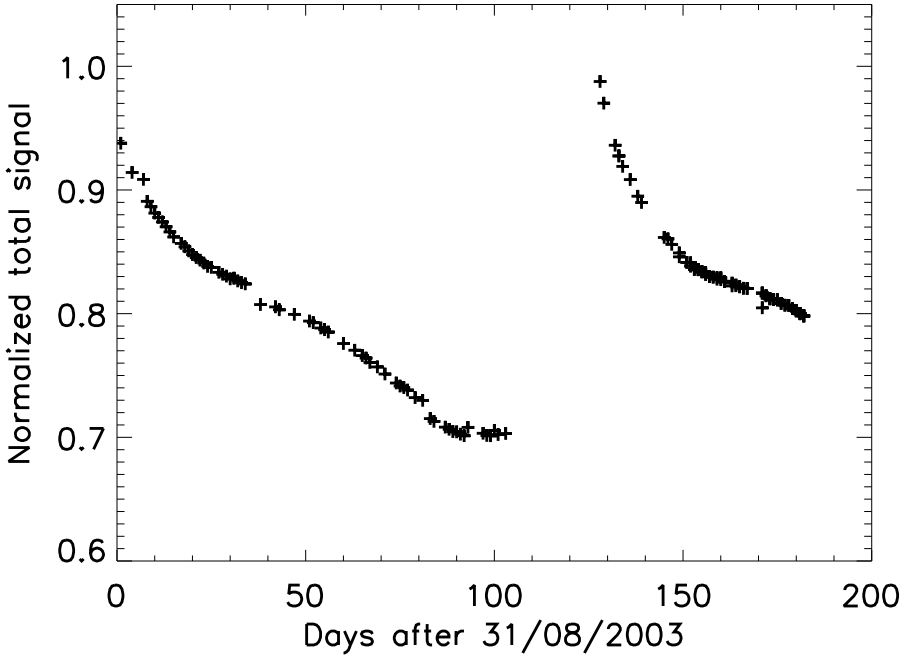

Fig. 2. The measured total signal averaged over channel 8 and normalised to an (almost) ice-free measurement in August 2002. Only data right after the August 2003 decontamination (duration: 375 h) till the end of February 2004 are shown and include the decontamination period in December 2003/January 2004 (duration: 338 h). The loss in the total signal due to the growing ice layer in SCIAMACHY's channel 8 can be clearly seen.

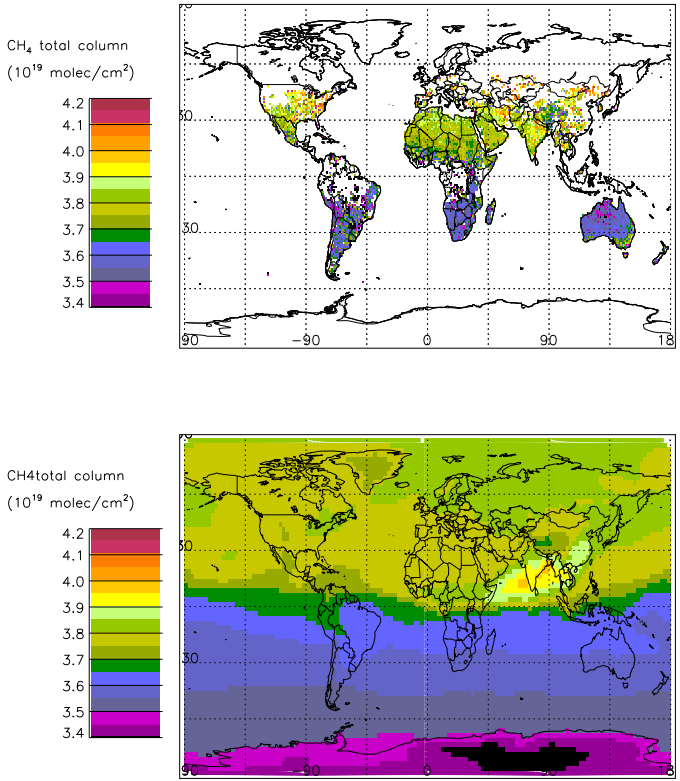

Fig. 3. Monthly averaged CH_4 total columns for November 2003. Top panel: Retrieval results from the IMLM algorithm. Only cloud-free individual SCIAMACHY ground pixels, with instrument-noise related errors $<0.2\times10^{19}$ cm^{-2} have been averaged and re-gridded on a $1^\circ\times1^\circ$ grid. The CH_4 total columns have been normalized to surface elevation prior to averaging. Bottom panel: Total columns calculated from the chemistry transport model TM3 on a 2.5° by 2.5° horizontal grid. The total columns have been normalized to surface pressure.

ACPD
5, 1733–1770, 2005

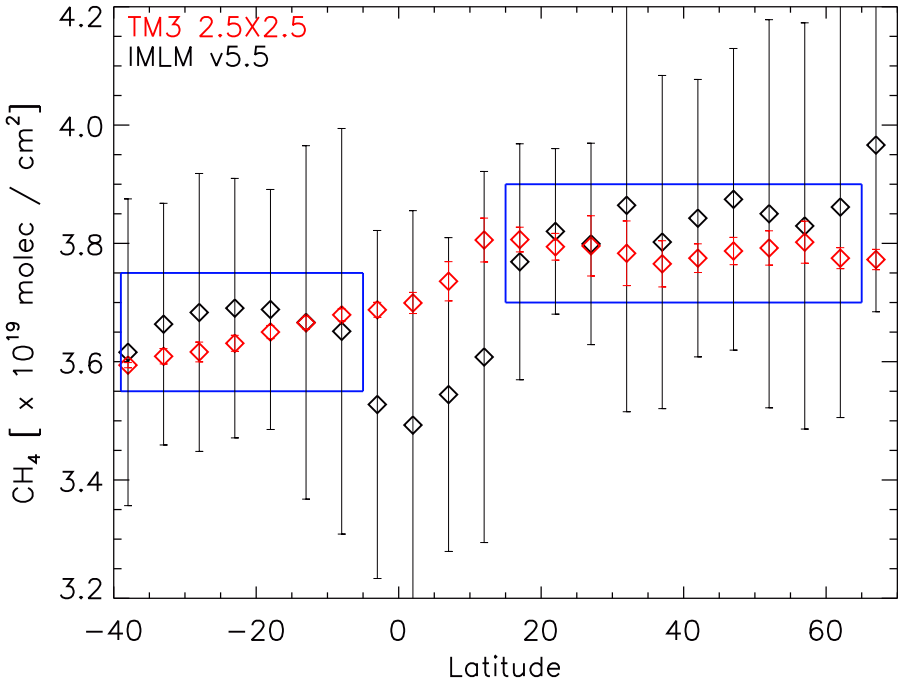

Fig. 4. Comparison of the monthly averaged CH_4 total columns for September 2003, where all data within a five-degree latitude bin have been averaged (see text). The black diamonds denote the IMLM CH_4 total columns, the red diamonds the corresponding TM3 data. The blue boxes show the regions where the difference between the IMLM and TM3 CH_4 total columns is $\lesssim$2%. Only cloud-free ground pixels with instrument-noise related errors $<0.2\times10^{19}$ molec/cm^2 have been included. The error bars denote the 1σ standard deviation of the data points averaged within each 5° latitude bin. Both the SCIAMACHY and the TM3 total columns have been normalized to the surface pressure.

ACPD
5, 1733–1770, 2005

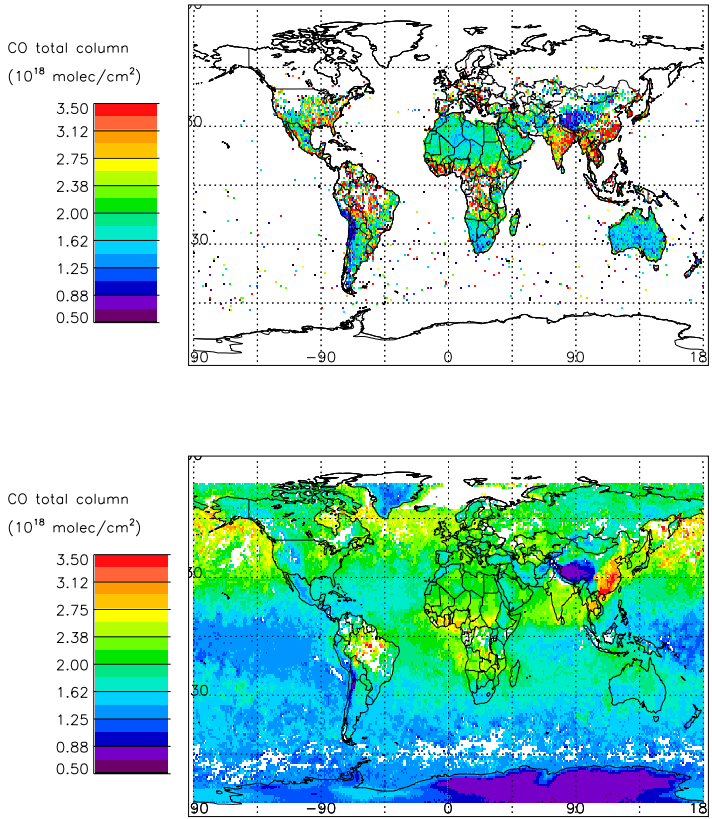

Fig. 5. Monthly averaged CO total columns for November 2003. Top panel: Retrieval results from the IMLM algorithm. Only cloud-free individual SCIAMACHY pixels, with instrument-noise related errors $<1.5\times10^{18}$ cm^{-2} have been averaged and re-gridded on a $1^\circ\times1^\circ$ grid. Bottom panel: Total columns as measured by the MOPITT instrument (from: NASA Langley Research Center Atmospheric Sciences Data Center). Only daytime measurements have been averaged.

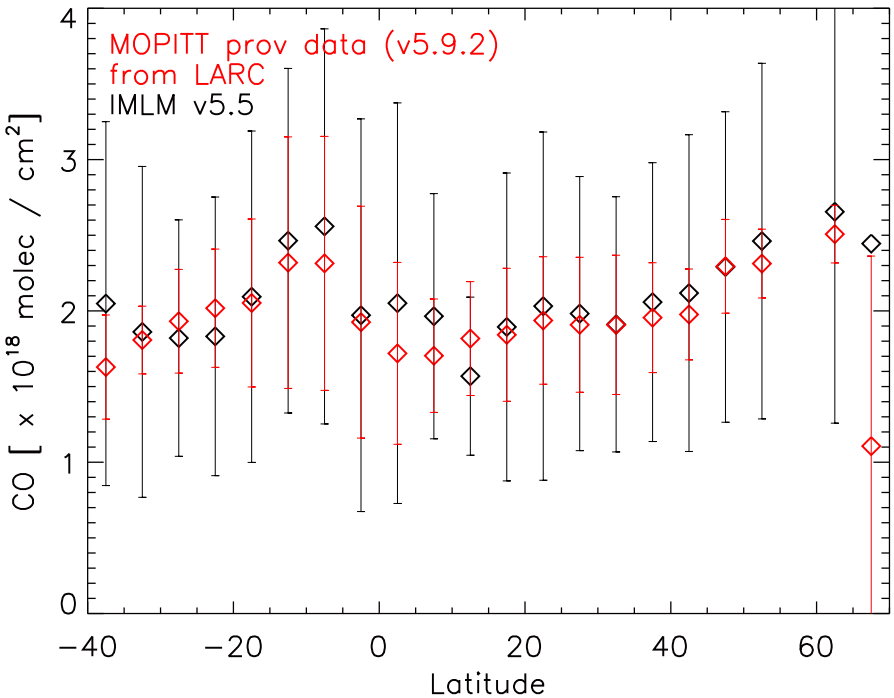

Fig. 6. Comparison of the monthly averaged CO total columns for September 2003, where all data within a five-degree latitude bin have been averaged. The black diamonds denote the IMLM CO total columns, the red diamonds the corresponding MOPITT data. Only pixels with a cloud-fraction <20% and instrument-noise related errors $<1.5\times10^{18}$ molec/cm^2 have been included. The error bars denote the 1σ standard deviation of the data points averaged within each 5° latitude bin. The MOPITT data are taken from the NASA Langley Research Center Atmospheric Sciences Data Center.

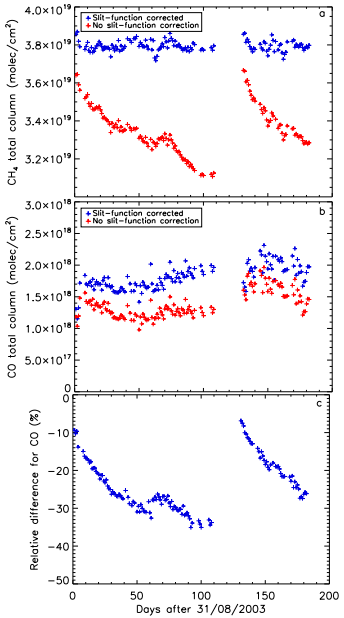

Fig. 7. Total columns averaged over the Sahara for each day in the period September 2003–February 2004, with and without applying a correction for the broadening of the slit function due to ice growth on SCIAMACHY's channel 8 detector (see Sect. 3). The gap between day 108 and 131 corresponds to the December 2003 decontamination period. **(a)** The CH_4 total columns, normalized to the mean surface elevation of the corresponding SCIAMACHY pixel and then averaged over the Sahara region. The trend seen in the CH_4 total columns without the slit-function correction resembles the loss in the total signal due to the ice growth in this period (Fig. 2). **(b)** The CO total columns. The columns without slit-function correction do not show a clear correlation with the decrease in the total signal for this period, but are nevertheless clearly affected by the broadening of the slit function. **(c)** Relative difference of the CO total columns without and with applying a slit-function correction respectively, as shown in panel b. The difference in the CO total columns clearly increases as the ice layer becomes thicker.

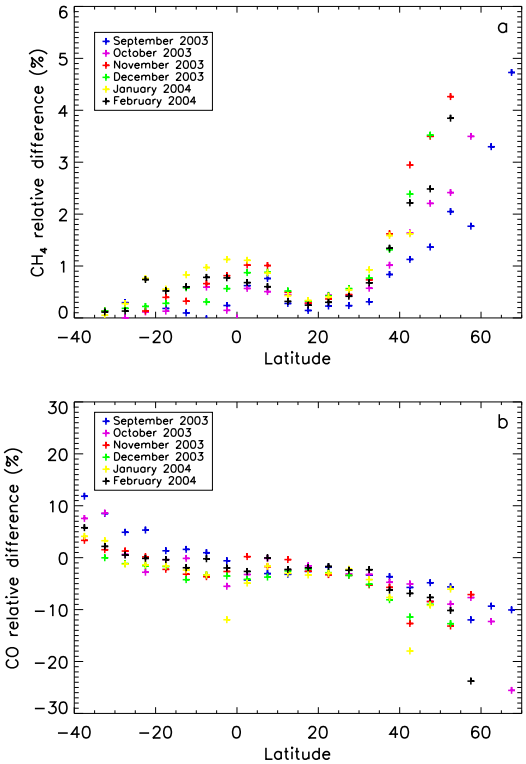

Fig. 8. The relative difference between the total columns retrieved without and with correction for the orbital variation of the dark signal respectively, for each month between September 2003 and February 2004. The data shown are the monthly mean total columns averaged per 5° latitude bin, between longitudes 30° W and 60° E. **(a)** The CH_4 total columns, normalized to the mean surface elevation of the corresponding SCIAMACHY pixel prior to averaging over a whole month of data. It is clearly seen that not correcting for the orbital variation of the dark signal leads to CH_4 columns that are up to ~4% too high on the Northern hemisphere. **(b)** The CO total columns, showing an effect opposite to that for CH_4.

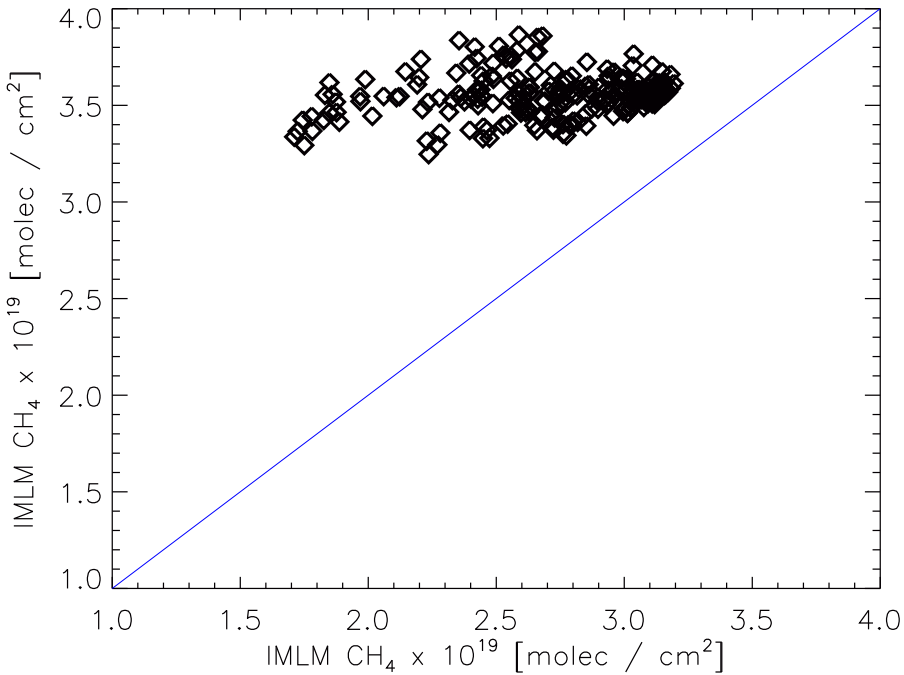

Fig. 9. The effect of 1 dead pixel on the CH_4 retrievals for orbit 10067 on 2 February 2004. The y-axis shows the CH_4 total columns when this dead pixel is not used in the retrievals. The x-axis shows the corresponding values when this pixel is included in the retrievals. The blue solid line denotes the expected 1:1 correlation. The deviation from the expected 1:1 correlation is different for each dead pixel (cf. Kleipool, 2004b).

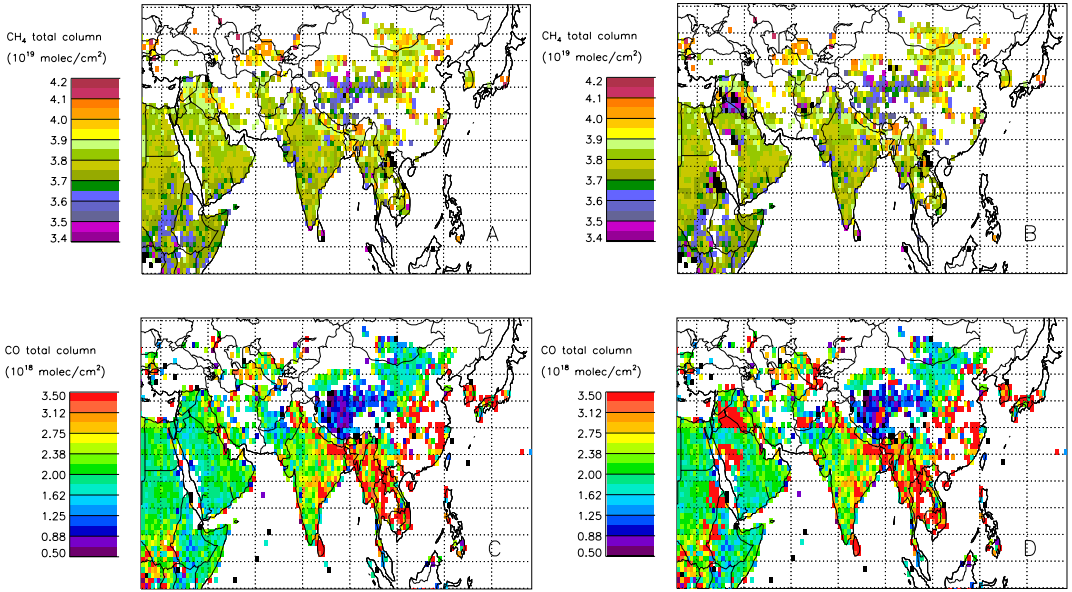

Fig. 10. Effect of not removing 1 dead pixel on the retrieved CH_4 and CO total columns over Asia and the Middle East for February 2004. **(a)** Monthly-averaged CH_4 total columns masking all dead pixels correctly. **(b)** Monthly-averaged CH_4 total columns omitting one dead pixel in the pixel mask for a period of 12 orbits (~0.85 day). **(c)** As panel a, but for CO. **(d)** As panel b, but for CO.